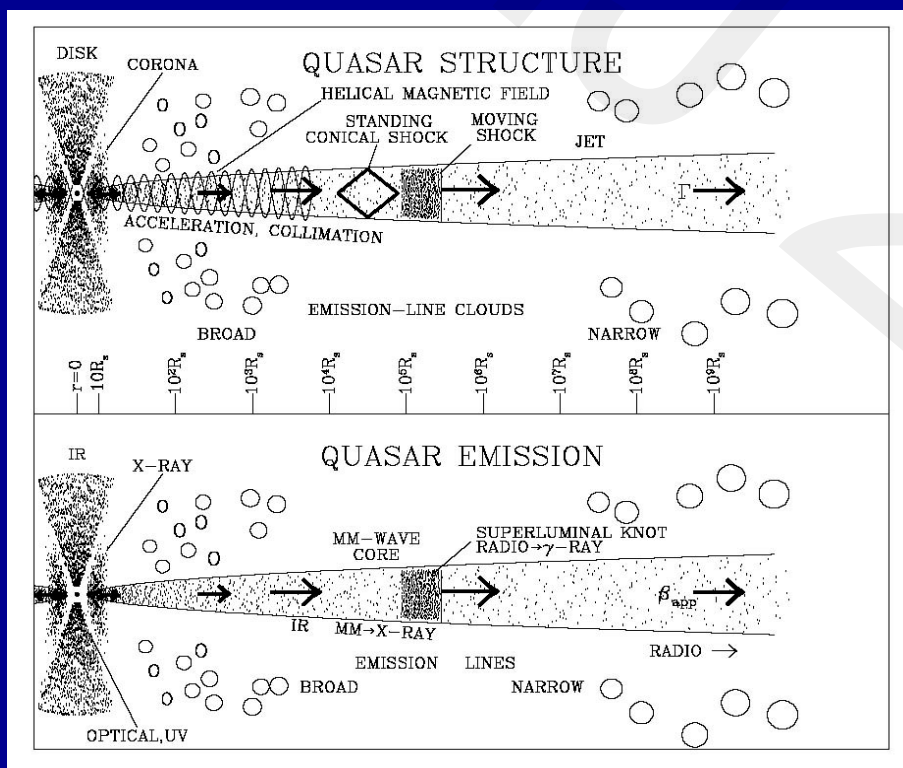
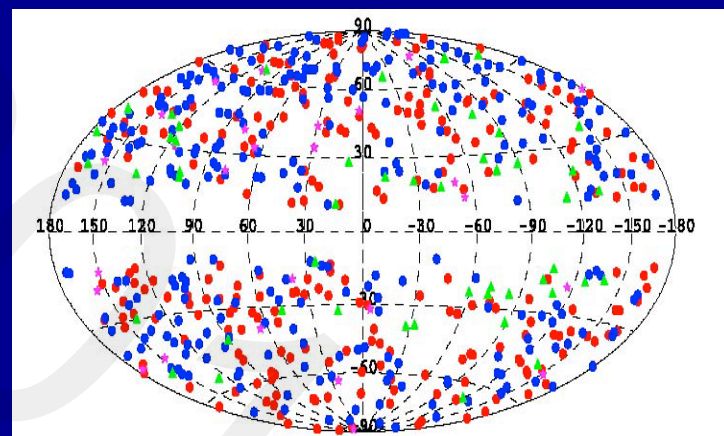


Probing the Physics of Gamma-Ray Blazars with Single-Dish Monitoring Data

M.F. Aller, P.A. Hughes & H.D. Aller (U. Michigan)



Marscher 2009



The γ -ray AGN distribution:
from the 11 month catalogue

Abdo et al. 2010

Outline

- ♣ Early results: the EGRET era
- ♣ Uses of Single Dish data in understanding Fermi photon flux data (light curves):
 - localization of the emission site
 - specification of the emission process
 - exploration of the role of shocks
- ♣ Future directions

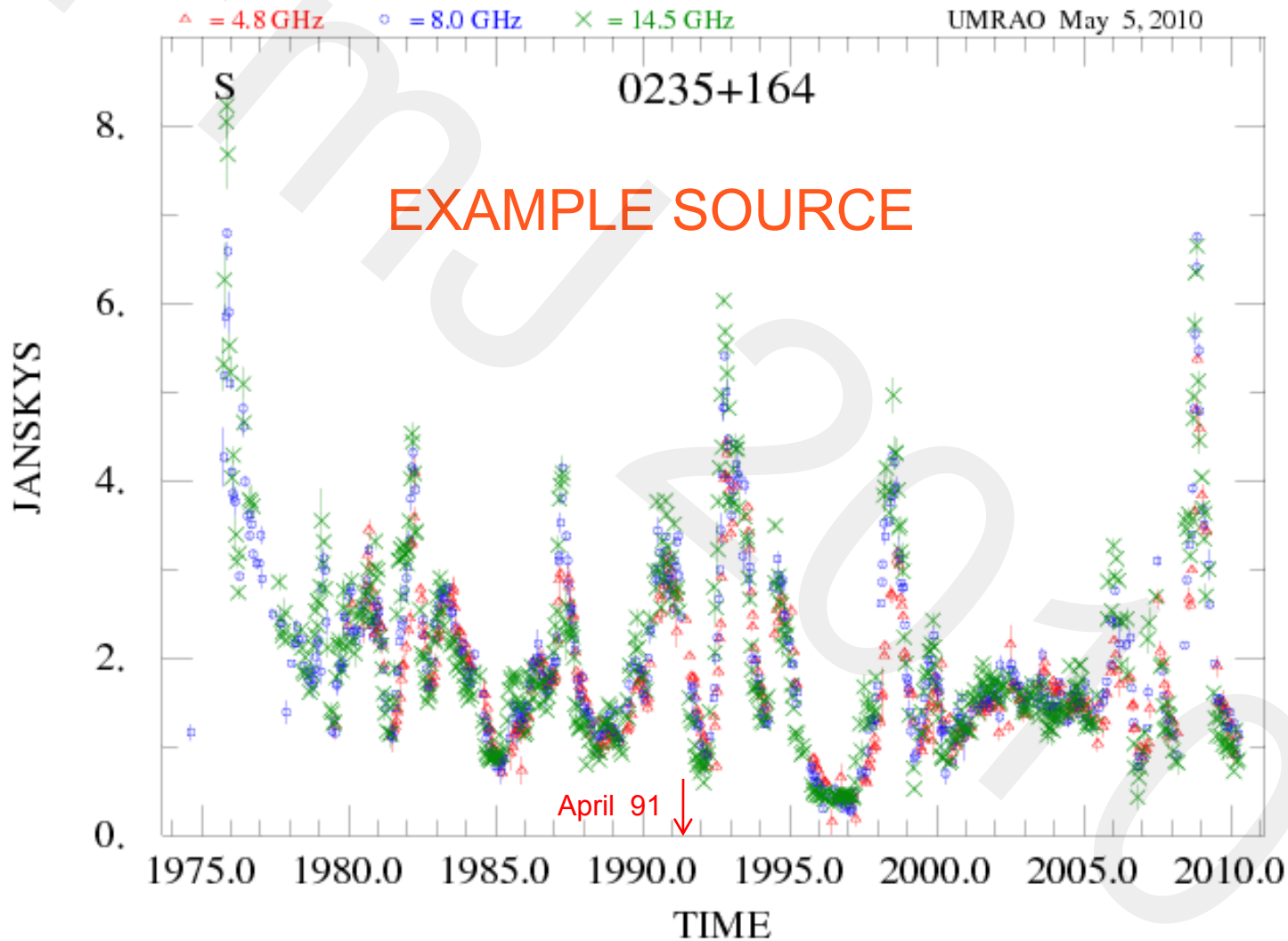
THE GAMMA-RAY DATA: EGRET DETECTIONS

The 1st EGRET Catalogue

TABLE 7
POSITIVE DETECTIONS ON RADIO-LOUD QUASARS AND BL LAC OBJECTS

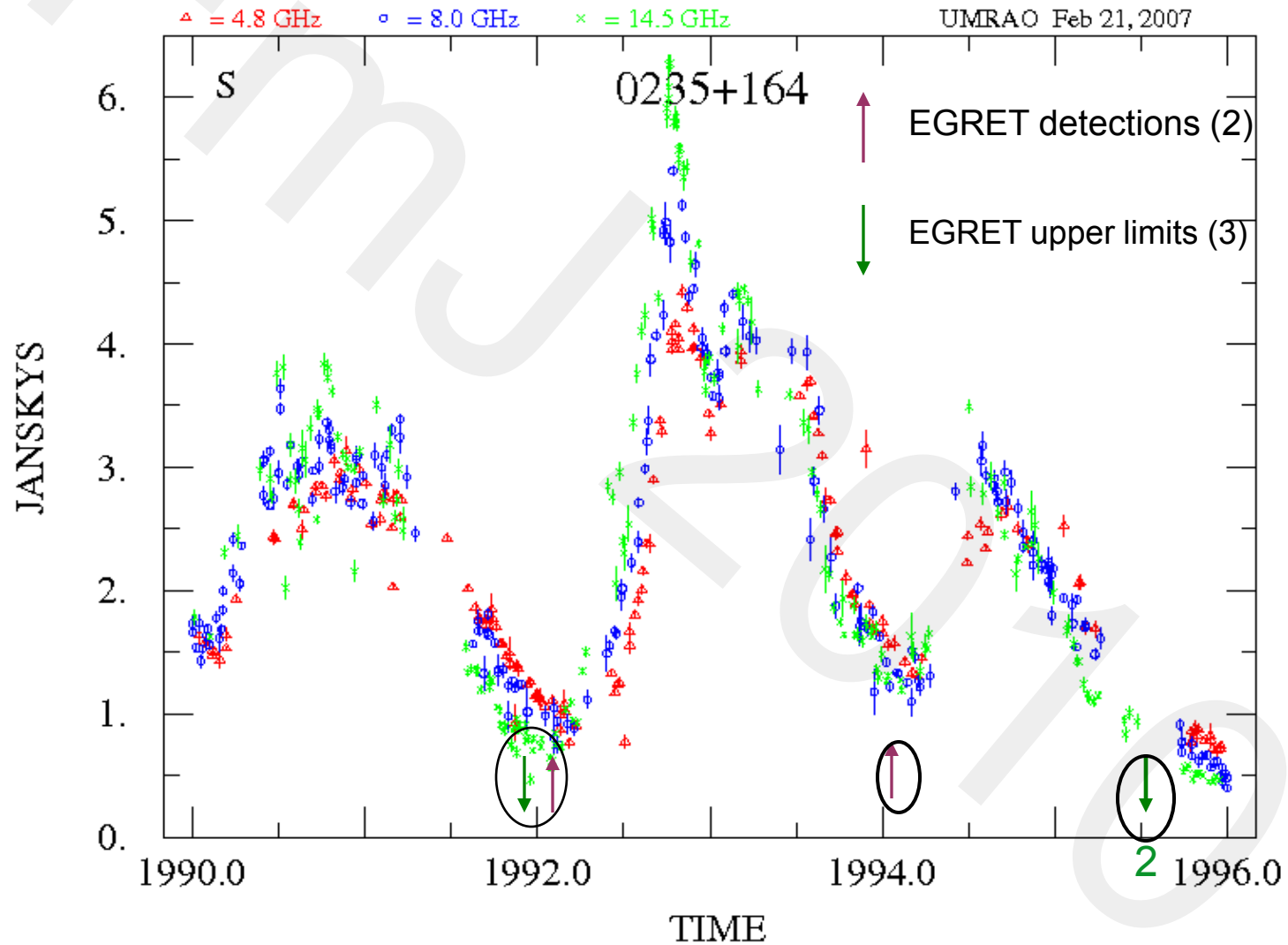
ID	Source ID and Characteristics						pos Diff. ^c	Pos Uncert. ^d	Flux ^e (10^{-6} cm ⁻² s ⁻¹) (E>100 MeV)	vp ^e	Photon Spectral Index	z	Rel Lumin ^f	Ref	Other Name
	OVV	BL Lac	Super Lum.	Radio Bright	Flat Radio ^a	Opt. Pol ^b									
0202+149				√	√	√	24	40	0.26±0.06 <0.5 0.26±0.05	21.0 26.0+28.0 Allsky	2.5±0.1			1	4C+15.05 PKS
0208-512				√	√	√	4	15	0.4±0.12 1.1±0.07 0.55±0.13 0.70±0.05	9.0 10.0 13.5 Allsky	1.7±0.1	1.003	2.1	2	PKS
0234+285			√	√	√	√	22	35	0.16±0.05 <0.6 <0.4 0.16±0.04	15.0 36.0-36.5 39.0 Allsky		1.213	0.4		4C 28.07 OD+258
0235+164		√	?	√	√	√	35	28	<0.3 0.82±0.09 0.48±0.05	15.0 21.0 Allsky	2.0±0.2	0.94	1.2	3	OD+160 PKS
0420-014	√			√	√	√	53	39	0.19±0.07 <0.14 <0.6 0.45±0.10 <0.3 0.19±0.04	0.2-0.5 1.0 2.5 21.0 29.0 Allsky		0.92		1	OA 129 PKS
0446+112				?	√		17	31	0.17±0.06 <0.16 <0.6 1.04±0.19 <0.5 0.19±0.03	0.2-0.5 1.0 2.5 36.0-36.5 39.0 Allsky	1.8±0.3				PKS
0454-463				√	√		20	71	0.29±0.07 <0.2 <0.2 <0.16 0.13±0.03	6.0 10.0 17.0 29.0 Allsky		0.858	0.3	1	PKS
0528+134	√			√	√		10	11	1.13±0.08 0.81±0.07 0.53±0.10 <0.6 <0.5 0.80±0.04	0.2-0.5 1.0 2.5 36.0-36.5 39.0 Allsky	2.6±0.1	2.06	8.0	4	PKS OG 147

THE RADIO DATA: LIGHT CURVES



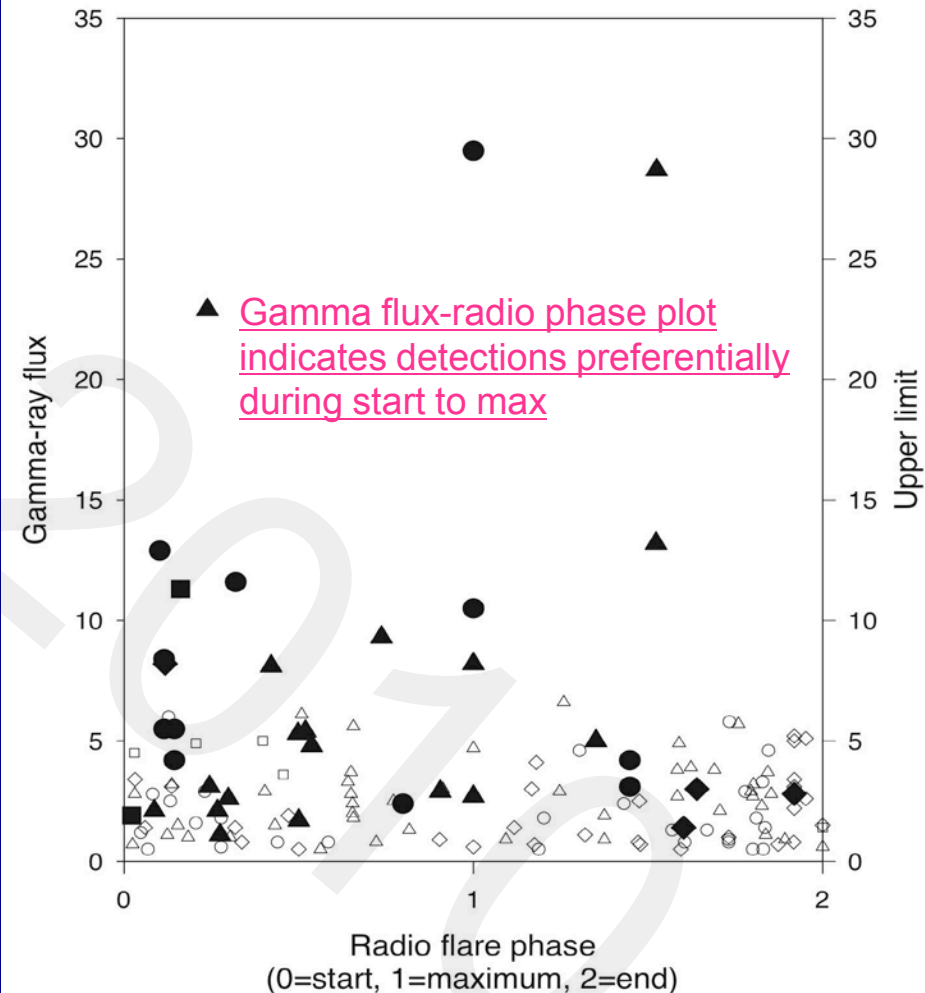
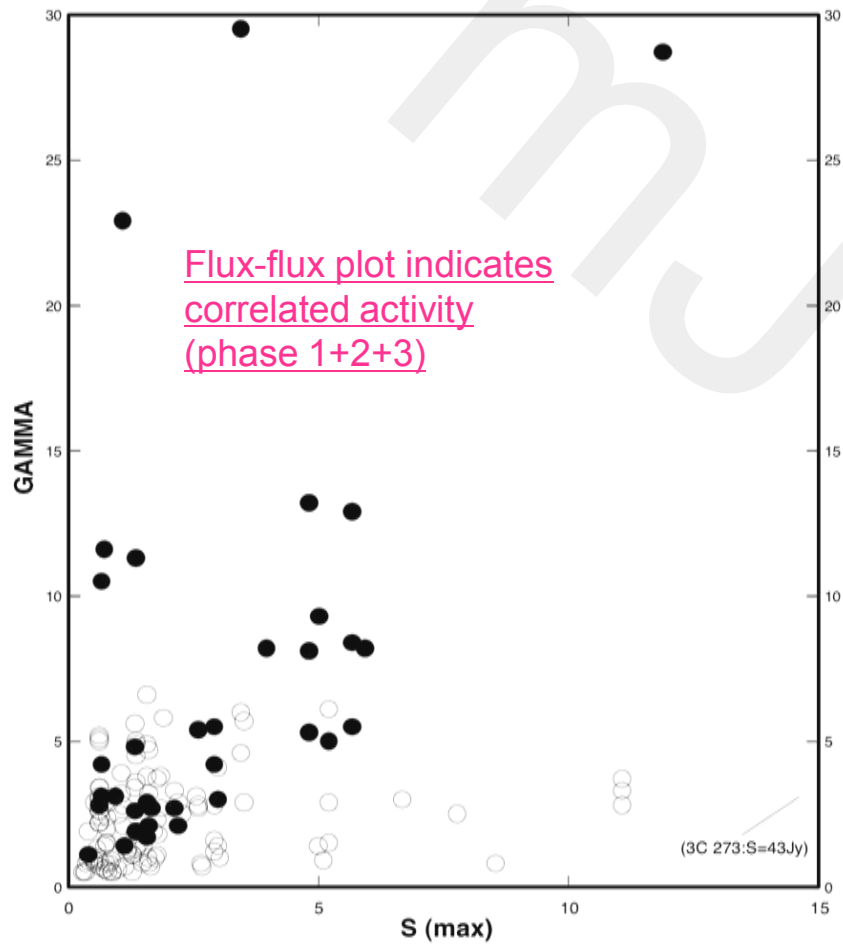
COMPARISON: Is This Activity Related?

Problem: limited sensitivity of EGRET & poor sampling

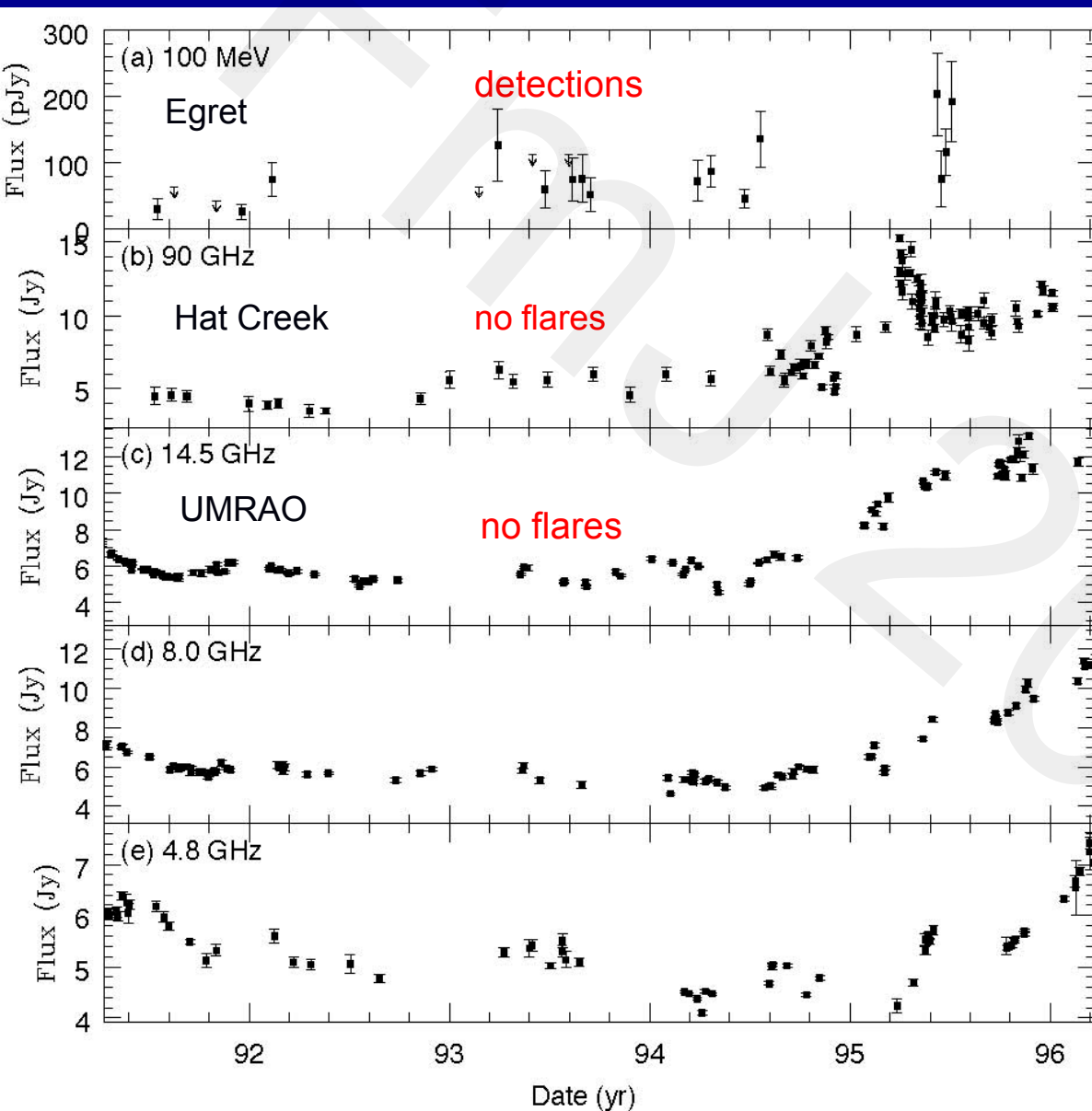


Statistical Evidence for Time-Correlated Activity

These correlations suggested that the same shocks produced the emissions in BOTH bands



NRAO 530: Detailed study of light curves



Gamma-ray detections do not always precede/match flares at mm/cm band: overall activity correlated but not specific flares

Global 1995 flux increase in all of the bands shown

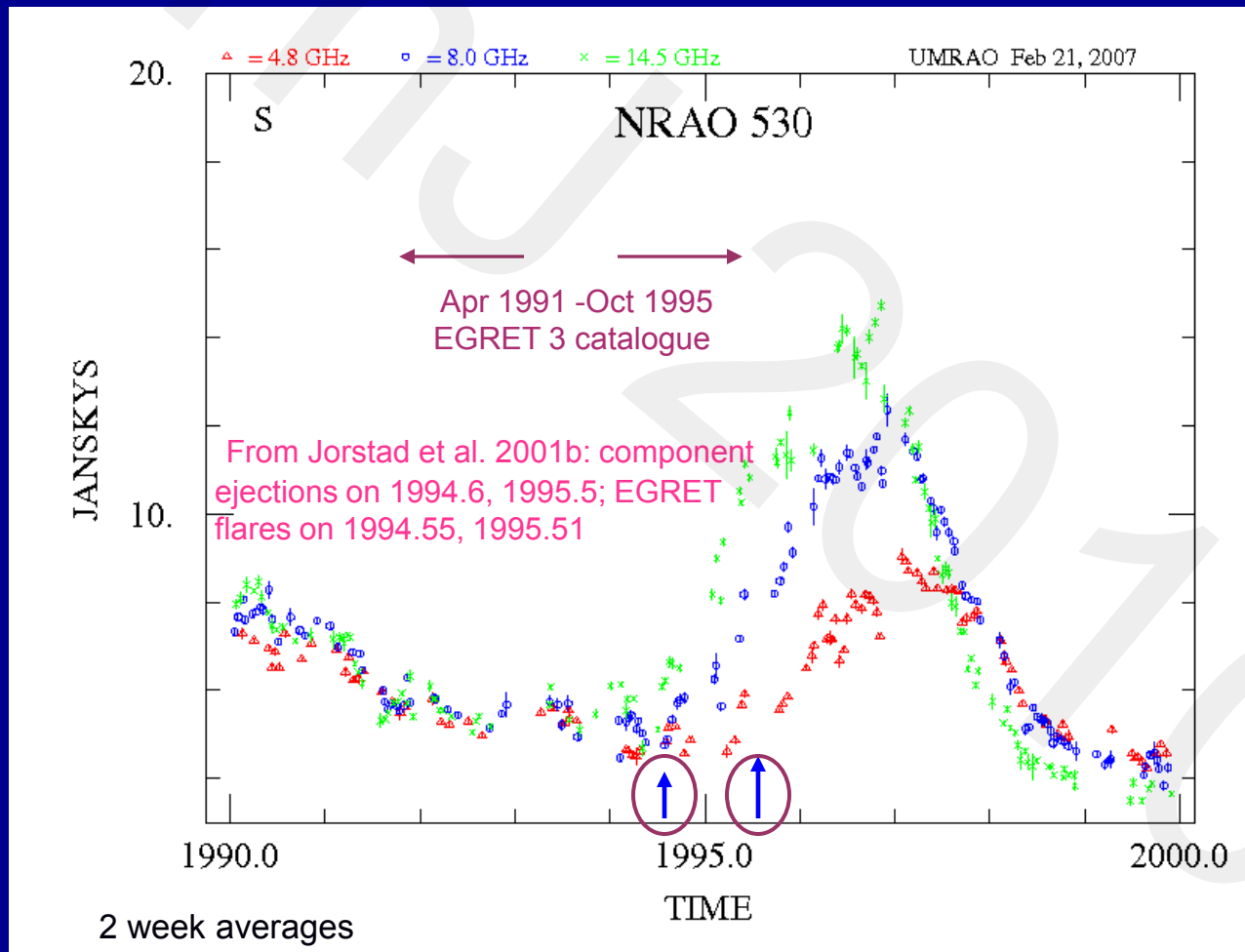
The activity is broadband suggesting that the same particles are responsible for the radio emission in the jet and the γ -ray emission.

New jet pc scale components evident in mm VLBI: 04/94, 04/95

EGRET + SD + VLBI monitoring

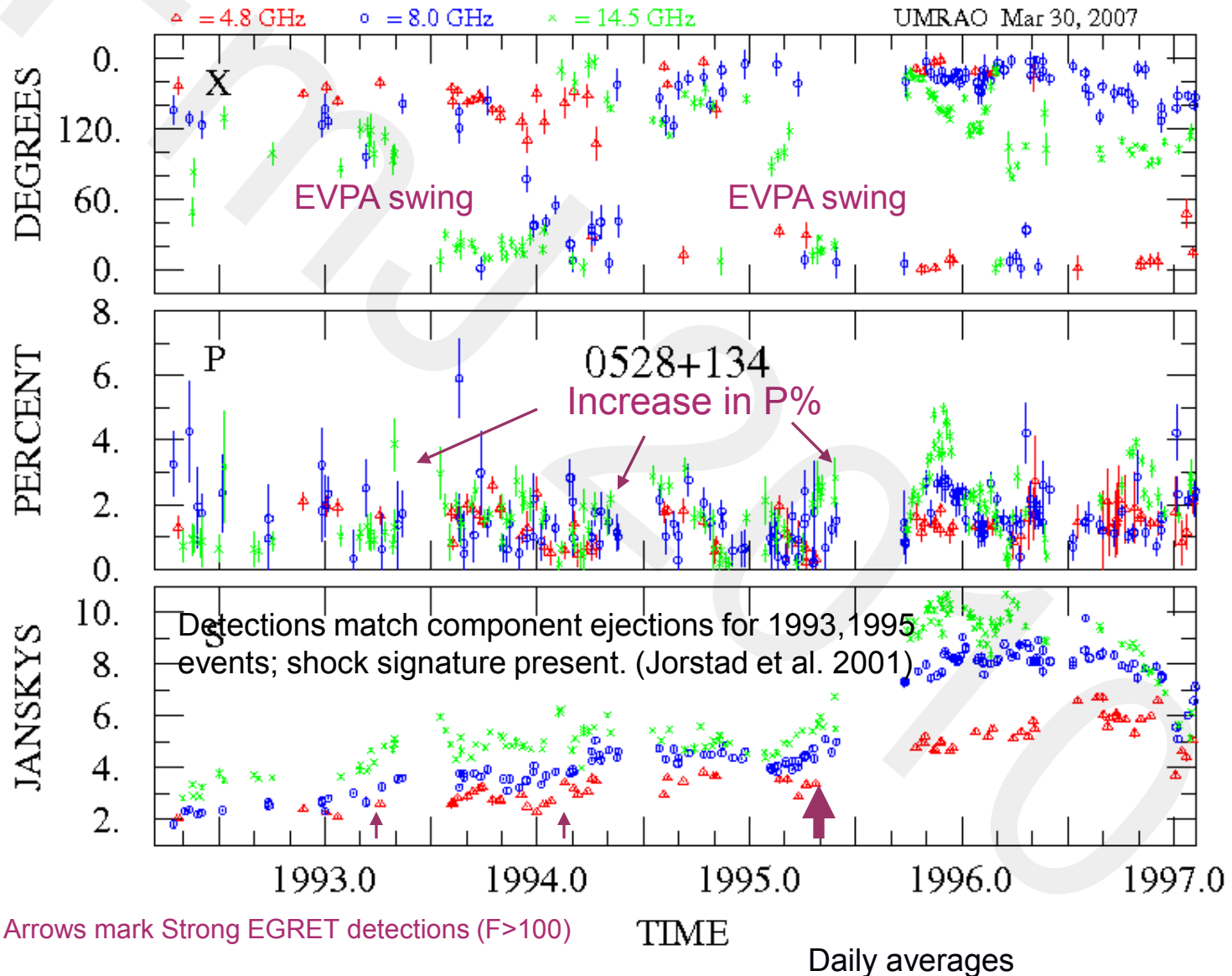
Temporal association between component ejection and flaring

VLBA monitoring data at 43, 22 GHz (Jorstad et al. 2001a,b) + epoch of flaring suggest that the γ -ray emission is produced by shocks downstream of the radio core



Linear Polarization as a Marker of Shocks in the Jet Flow

The temporal association between EGRET detections, new VLBI components, & changes in LP indicate that internal shocks play a role in the generation of the gamma-ray emission.



Questions to be answered in the Fermi era

- ☞ Where within the jet* is the γ -ray emission produced? (localization of physical site using light curves)
- ☞ What is the emission mechanism? (character of the variability from studies of the distribution of power; SEDs)
- ☞ What is the mechanism for the acceleration of particles? (tests for the presence of shocks during gamma-ray flaring)
- ☞ What special conditions are present in the jet during broad band flaring? (identification of jet properties during flaring and of changes in jet conditions from flare to flare)

* Rapid variability in some sources suggests an emission site near the central engine but see Marscher and Jorstad paper this meeting.

Current monitoring programs

Program	Frequency (GHz)	sampling	Size/advantage
OVRO	15	2-3/week	>1150 many sources: low S
Effelsberg	2.64 - 43	monthly	≈60 spectra
IRAM	86 - 270	monthly	≈ 60 inner jet
UMRAO	4.8, 8.0, 14.5	1-2/week	35 in core group mf; includes LP
Metsähovi	37	monthly	≈100 inner jet
RATAN-600	1-22	2-4/year	600 spectra

The combined data provides both temporal and spectral coverage.

Evidence for correlated activity: *Fermi* + MOJAVE + SD

Time-averaged data for 77 MOJAVE sources in 3-month bright AGN list

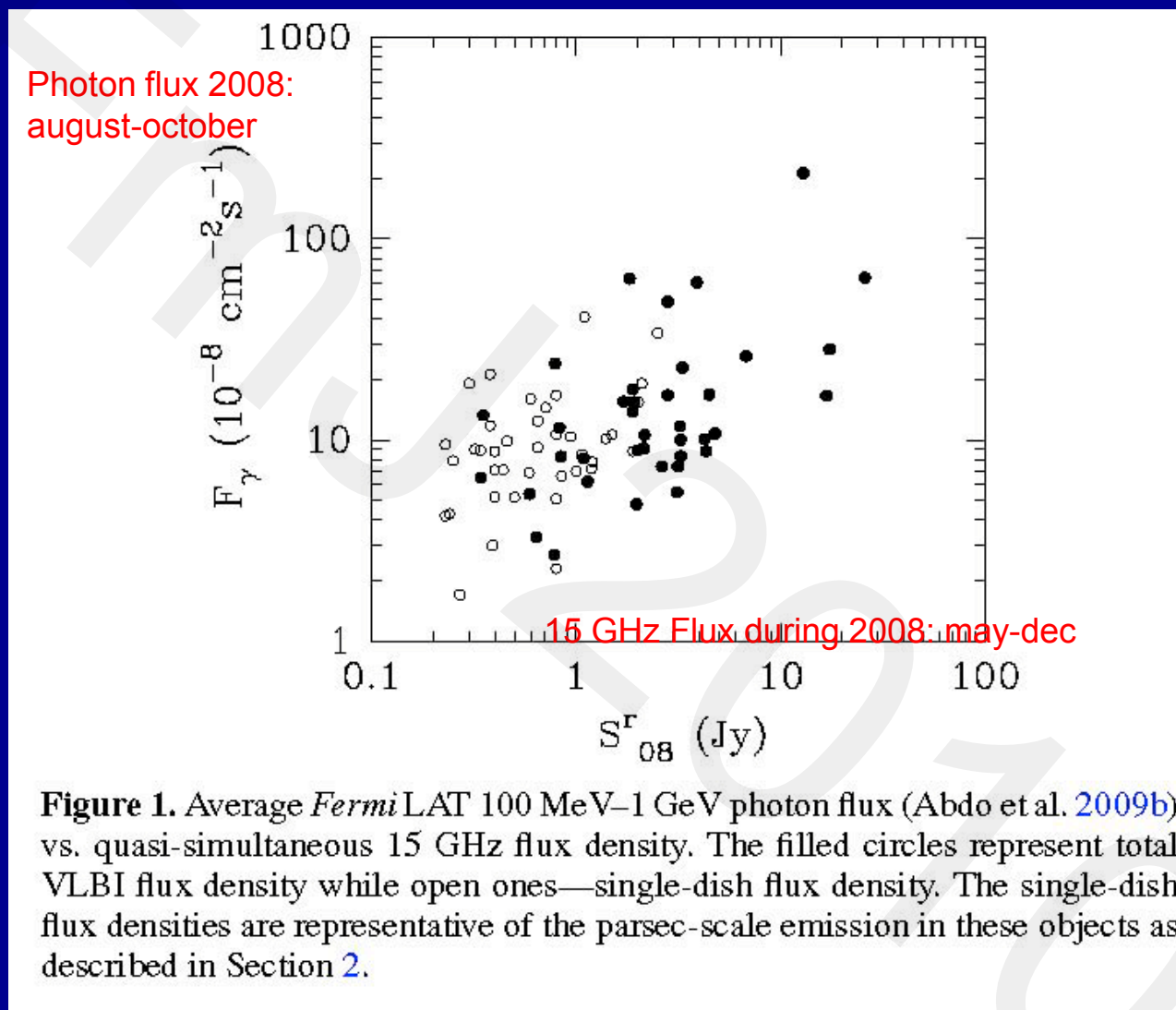


Figure 1. Average *Fermi* LAT 100 MeV–1 GeV photon flux (Abdo et al. 2009b) vs. quasi-simultaneous 15 GHz flux density. The filled circles represent total VLBI flux density while open ones—single-dish flux density. The single-dish flux densities are representative of the parsec-scale emission in these objects as described in Section 2.

Result: A high-confidence positive correlation is found using a statistically complete sample.

Radio band – Gamma-ray Correlations

OVRO versus *Fermi* flux density; time-averaged data for 49 sources with known redshift in the 3 month bright AGN list

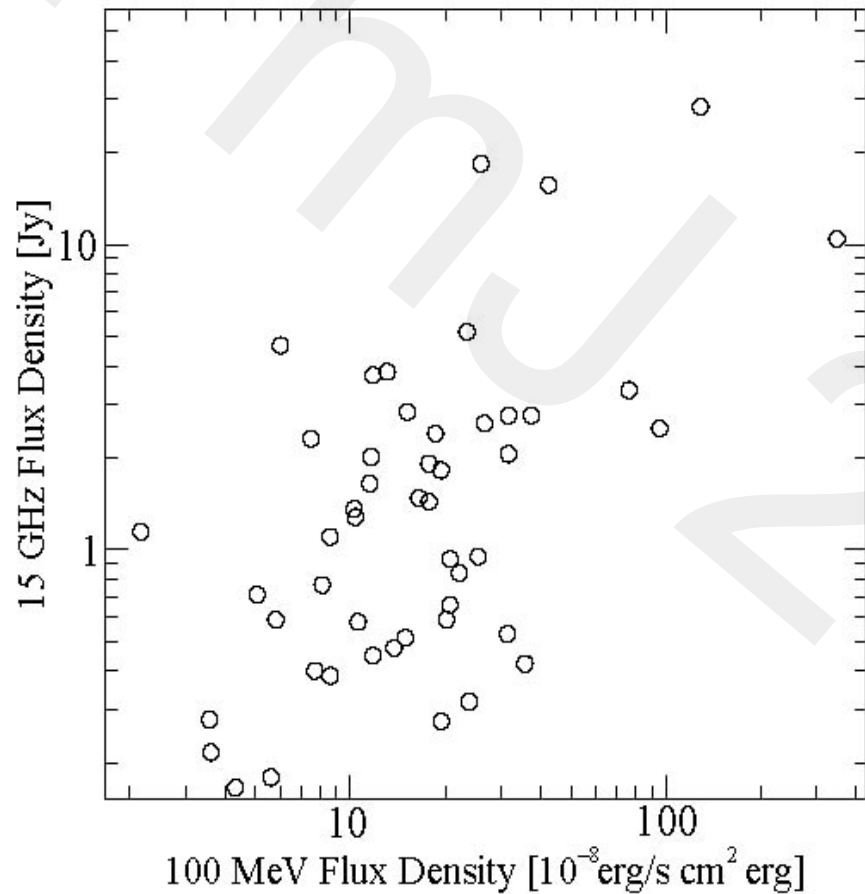


Figure 6: OVRO 15 GHz flux density versus *Fermi*-LAT 100 MeV flux density.

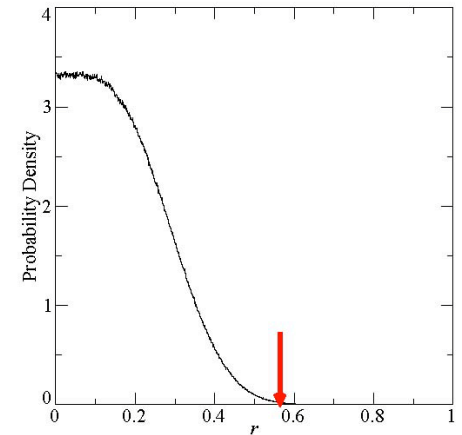


Figure 7: Monte Carlo-estimated probability density function for the correlation coefficient, r , between OVRO 15 GHz and *Fermi* 100 MeV flux densities. Arrow indicates measured value.

Correlation coefficient=0.56;
Chance probability= 5×10^{-4}

LIGHT CURVES: localization and emission process

Source Property

lags, leads (localization)
Time scale, noise process
Degree of variability

Periodicity

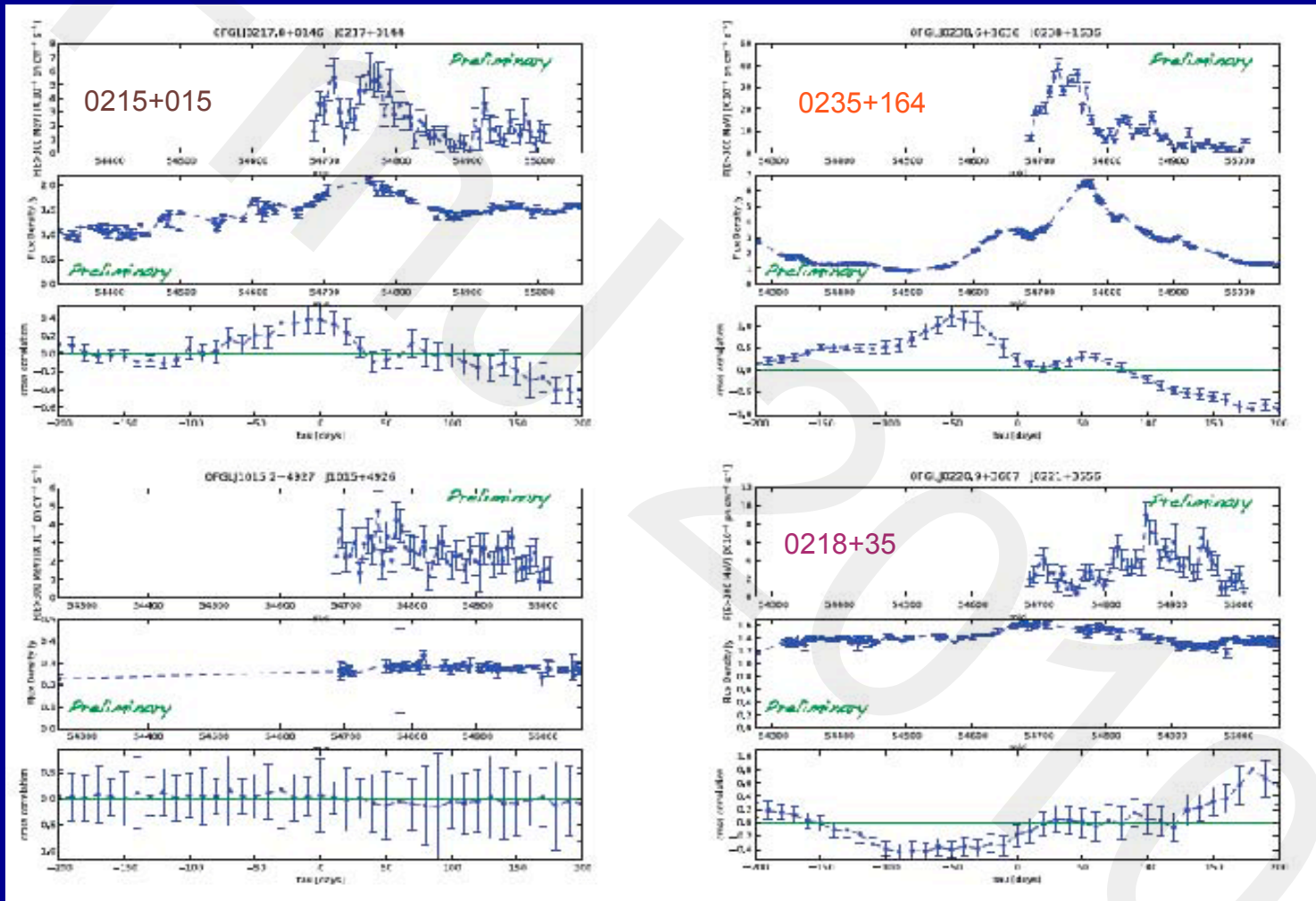
Length of data trains:
radio: up to 4 decades

Common Method

Cross correlations
Structure functions
FI, normalized excess
variance
cross-wavelets

gamma-ray: 2years

Cross-Correlations of Fermi & OVRO Light Curves



Fermi

OVRO

Lag

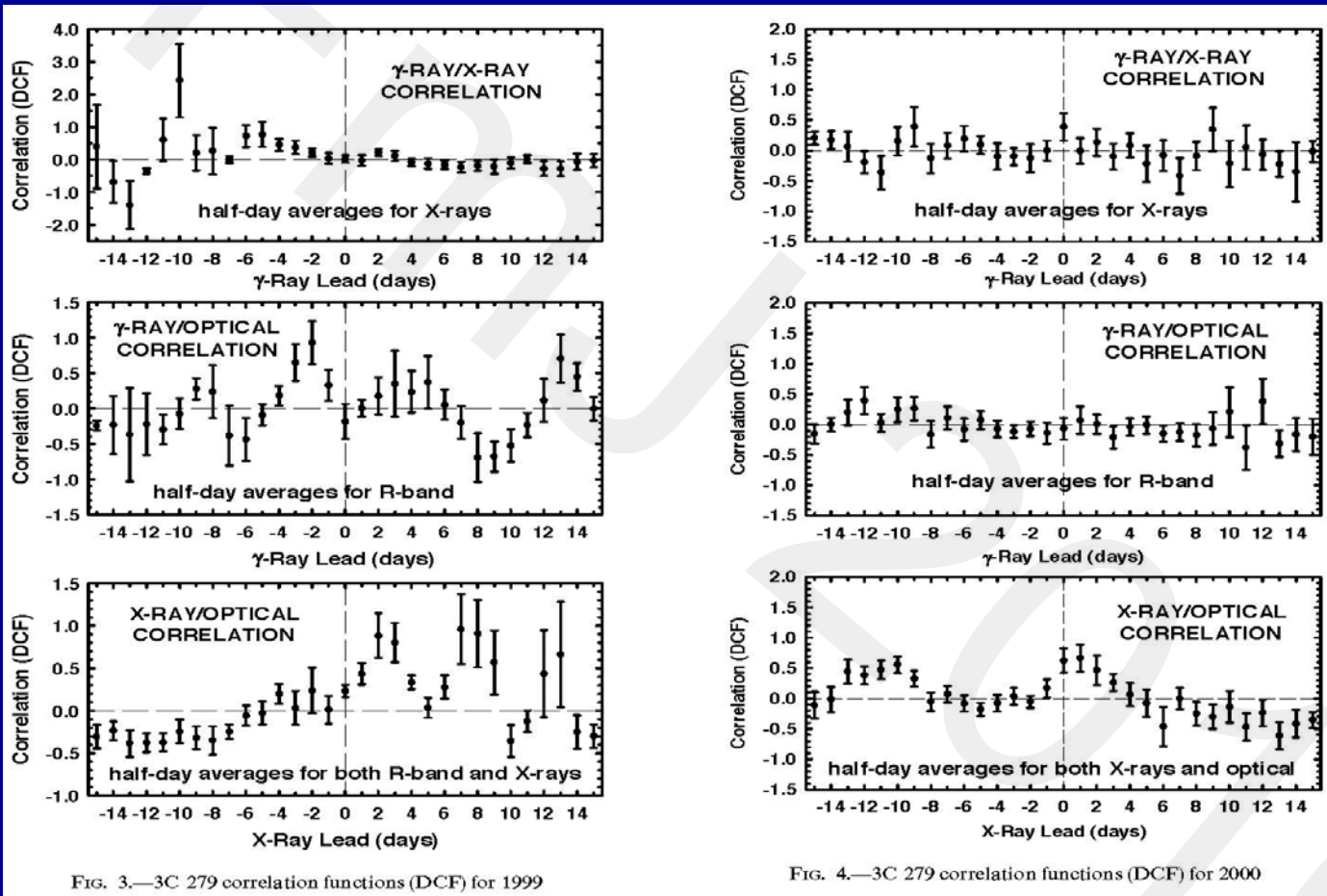
RESULT: A variety of patterns is found based on these short data trains. (top two shown dominated by a single event; gamma leads radio)

Inherent Problems in Using Cross-Correlations of Light Curves for Localization:

- ♣ Unambiguous identification of the SAME event is difficult except when the light curve is dominated by a single event (e.g. 0235+164).
- ♣ Self-absorption and opacity produce delays.
- ♣ A `long' data train is required to capture the full range of behavior which can change from epoch to epoch
- ♣ Changes in the parameters regulating the emission as a function of waveband may change with time

Inter-band TIME LAGS

EGRET result for 3C 279



Patterns change with time in the same source. (No persistent trends in general.)

RESULT: Time-dependence may reflect variations in input parameters (Böttcher and Dermer 2010).

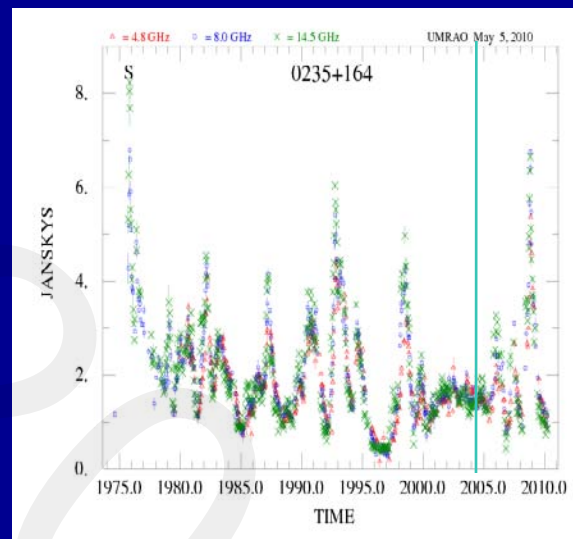
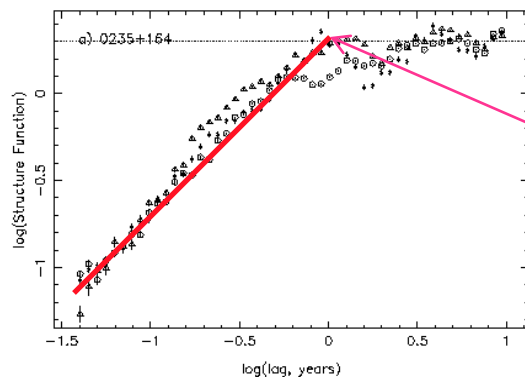
Characterization of the Emission:

timescales & noise process from 1st-order structure function analysis

STRUCTURE FUNCTIONS

$$D(\tau) = \langle [S(t) - S(t + \tau)]^2 \rangle \\ = 2\sigma^2(1 - \rho(\tau)) \text{ for stationary noise}$$

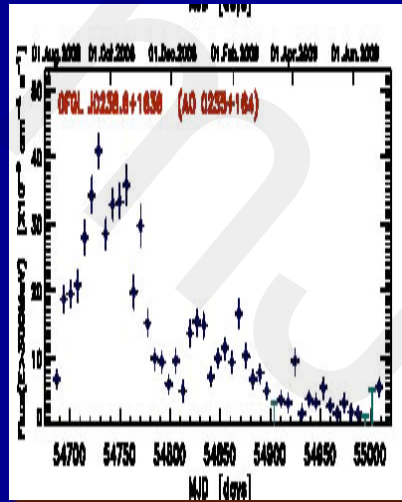
$\{ D \propto \tau^a \leftarrow \text{"measures" process}$
 $\{ \tau < \tau_c \leftarrow \text{measures correlation time scale}$



Turnover gives the maximum correlation time scale. Using data thru 2005, $\tau=0.87$ yrs; $\tau/(1+z)=0.45$ yrs. The value obtained can be a function of the time window.

Slope 'measures' noise process.

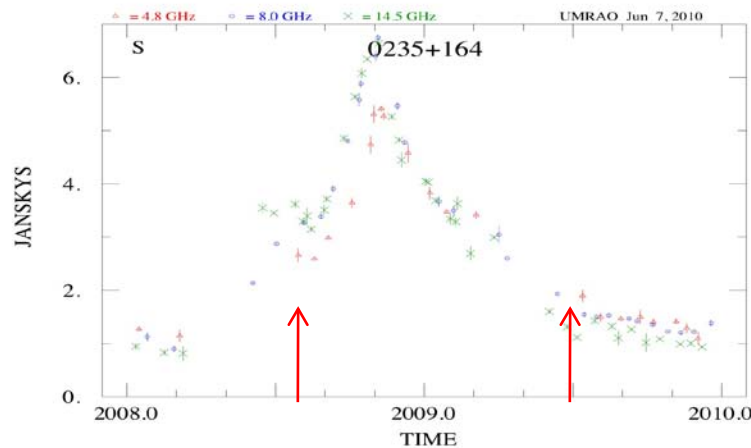
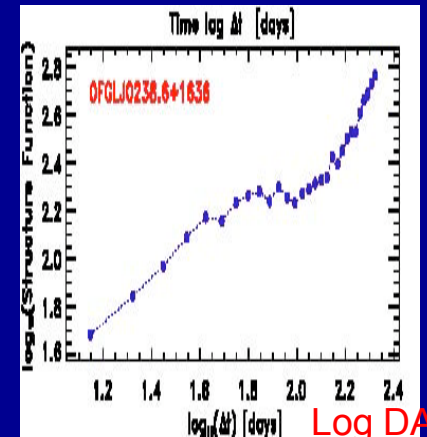
Character of the Variability During the First 11 months of Fermi Operation 08/04-2008 – 07/04/09



Fermi: $E > 300$ MeV;
1 week average

Dominated by a single 'event'

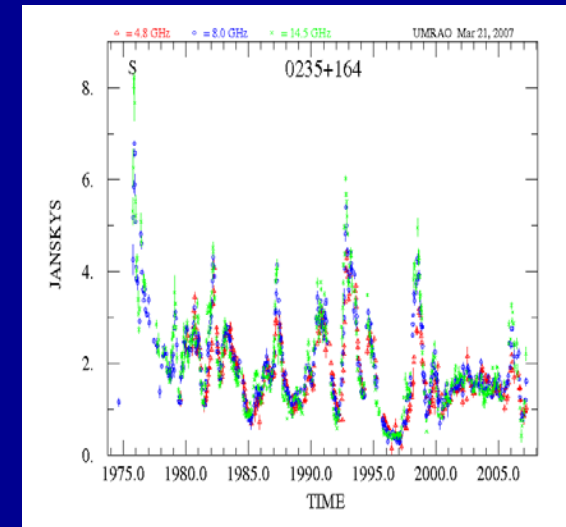
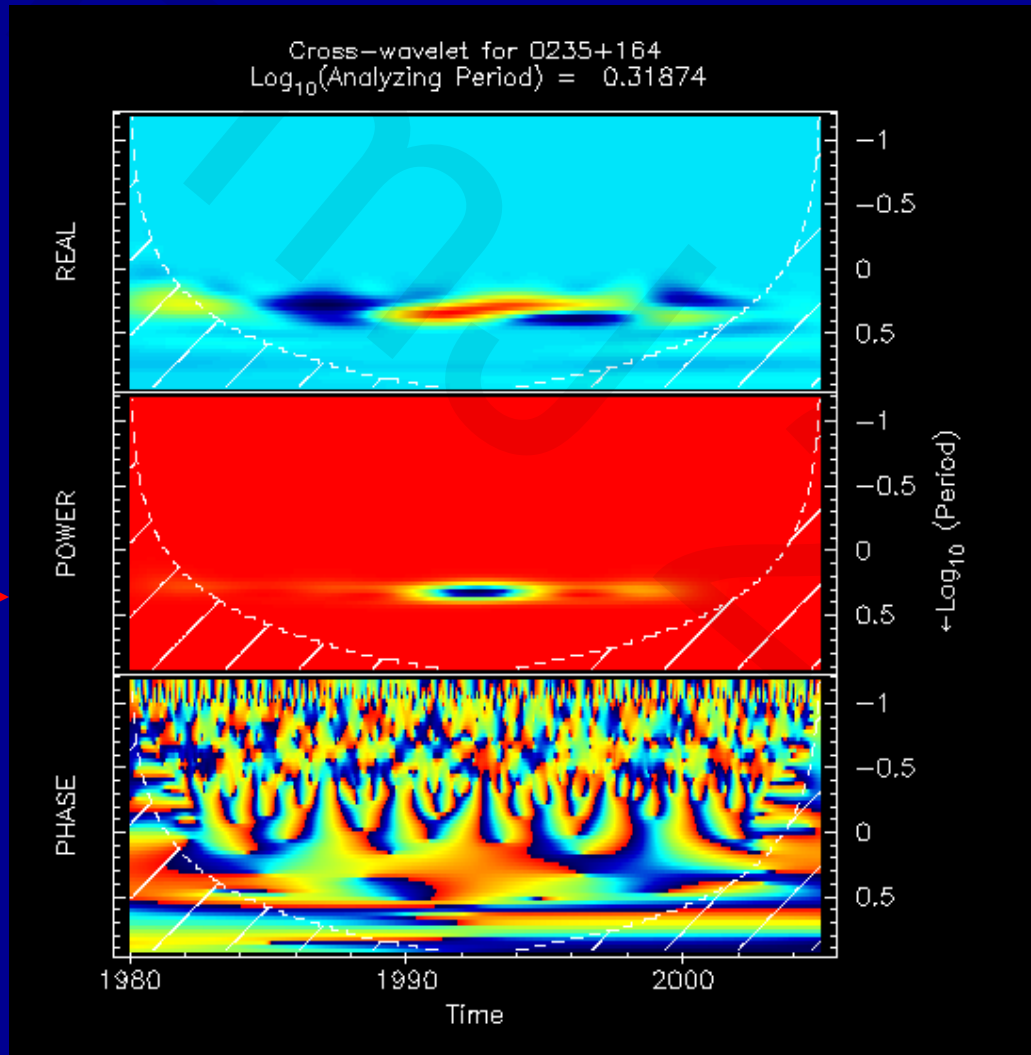
Fermi SF for
0235+164



Cm-band: 4.8-14.5 GHz:
1 wk average

Dominated by a single event but timescale longer

Results from Long-term UMRAO Data: quasi-periodic behavior (wavelets, cross-wavelets)



Result: 1.9, 2.7 years

Independent analysis of 25 years of optical + radio data (Raiteri et al. 2001) gave $P=5.7 \pm 0.5$. Next event did not follow expected pattern

Radio band: Different methods identify different 'periods': all are yrs.

Are Similar Emission Properties Apparent?

♄ Slope of SF (noise process): 0235+164 and 3C 454.3 dominated by a single event in BOTH bands in Fermi era. In general: radio band $b=1$ (shot noise), in gamma band $b \approx 0.0$ (white noise) sometimes

♄ Characteristic times scales:

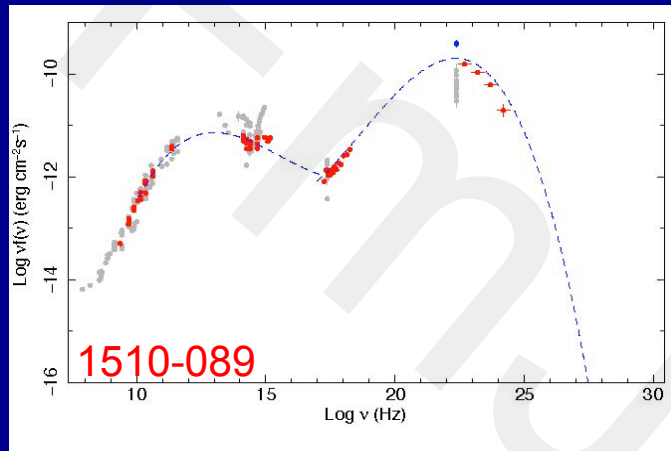
$\tau \approx 2$ years at cm band (from SF analysis).

$\tau \approx 7$ weeks at gamma ray band (from DACF lag times). different

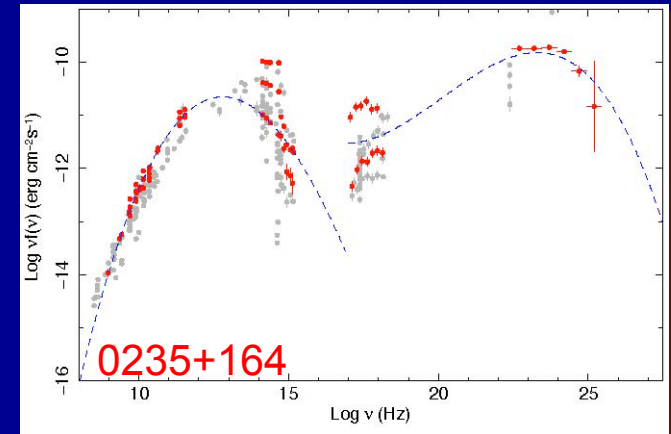
♣ Periodicity:

quasi periodicity in several sources $>$ year at radio band. None yet at gamma ray band. OJ 287 best case in radio. don't know yet

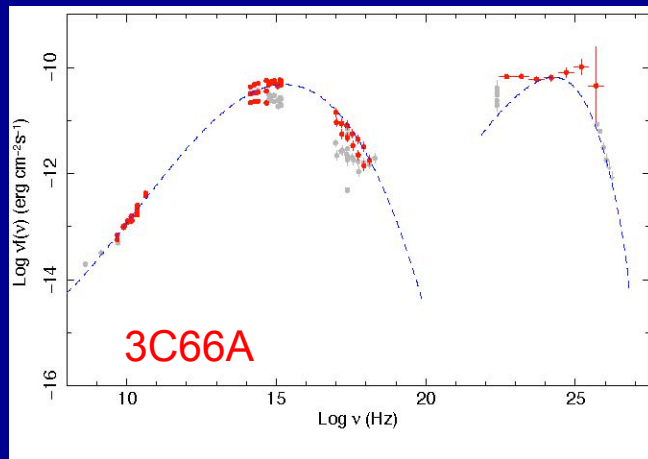
Characteristic SEDs: study of the relation of SSC and IC components using quasi-simultaneous data (Aug-Oct 08)



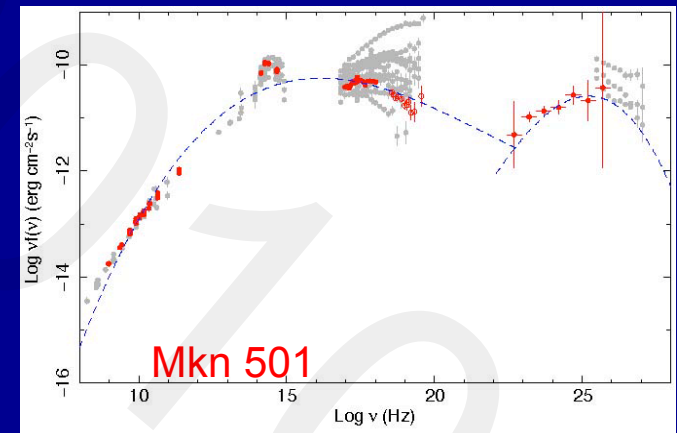
LSP FSRQ Compton Dom.=7.4



LSP BL Compton Dom.=1.5



ISP BL Compton Dom.=1

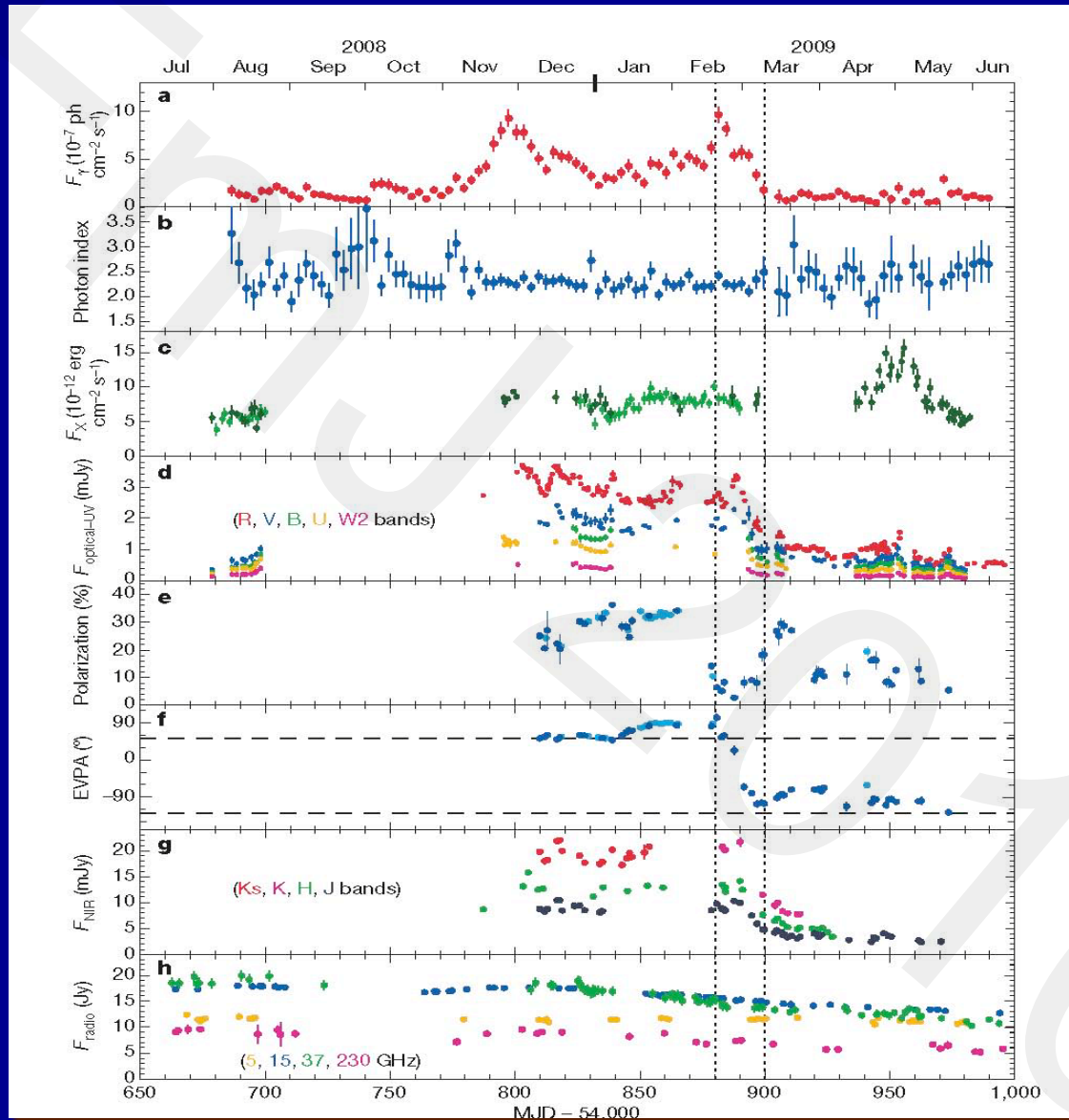


HSP BL Compton Dom.= 0.5

Analysis uses SD monitoring data

Abdo et al. submitted

Evolution of the SED: 3C 279 During Activity



Gamma: Flaring

X-ray

Optical

NIR

Radio: monotonic decrease

RESULT: The Mf behavior is complex.

Abdo et al. 2010

Evolution of the SED During γ -ray Flaring

Evolution of the SED during a single 'event'

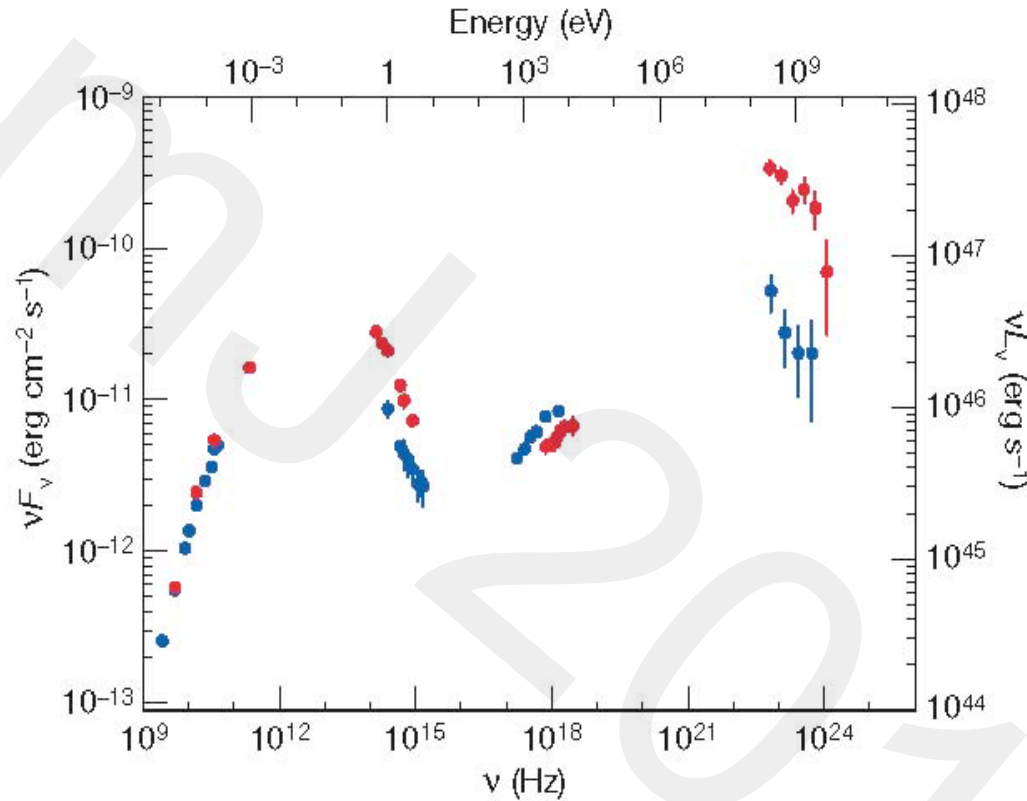
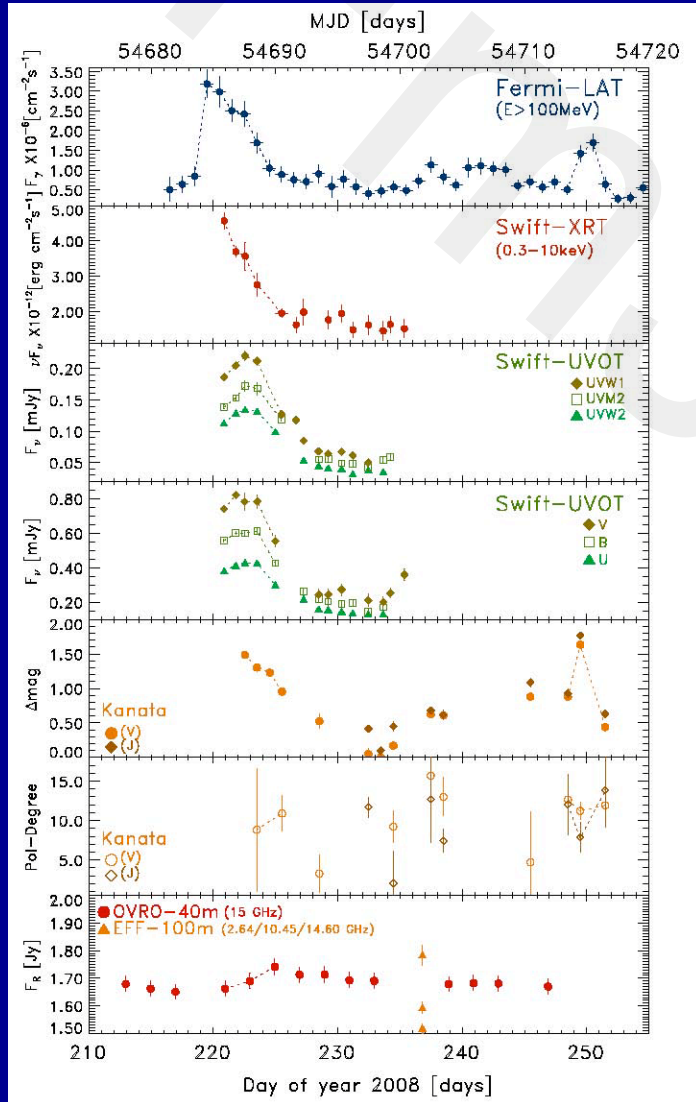


Figure 2 | Energy spectrum from radio to γ -ray band of 3C 279 at two different epochs. The red points were taken between 54880 and 54885 MJD, corresponding to the first five days of the sharp γ -ray flare accompanying the dramatic polarization change event (epoch 1). The blue points were taken between 54950 and 54960 MJD, around the peak of the isolated X-ray flare

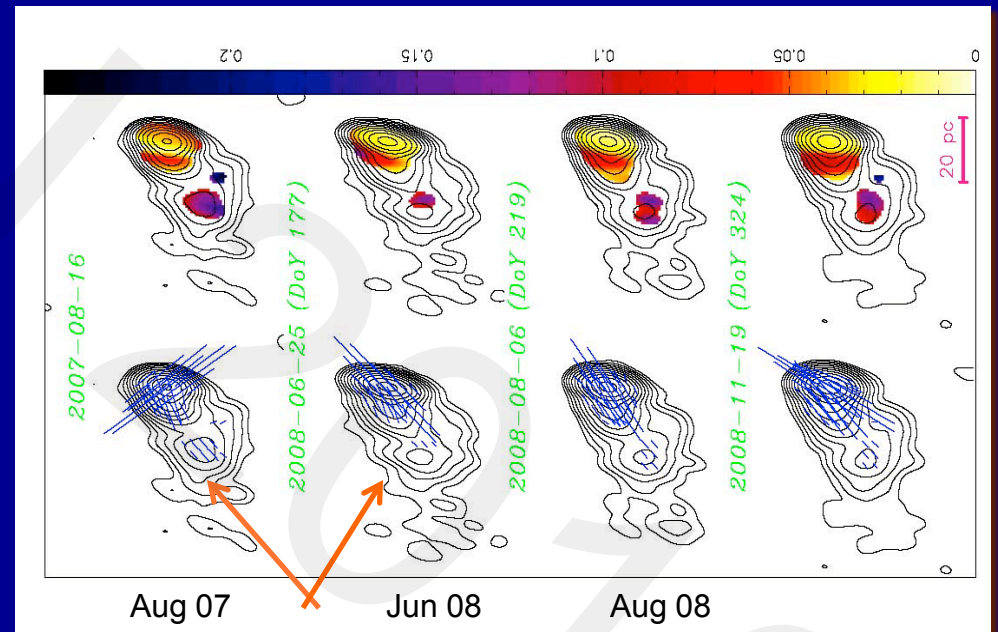
RESULT: significant changes are present in all bands except the radio.

SHOCKS: A Mechanism for Particle Acceleration

August 2008 event: 1502+106

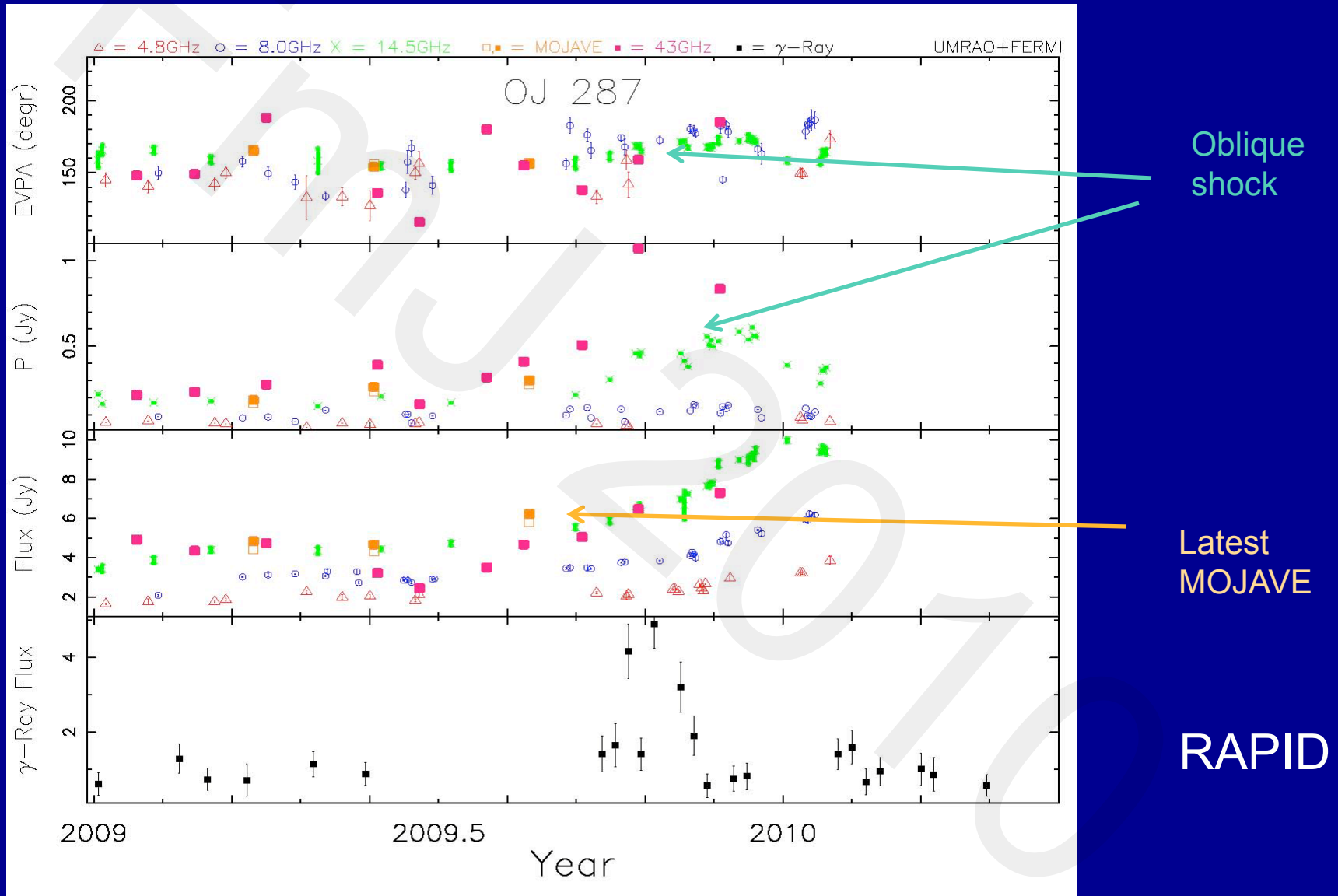


Evidence for shocks during flaring from MOJAVE VLBP measurements: 1502+106



EVPA swing

Example of Shock Signature in LP data



Description of UMRAO Oblique Shock Models (evolution of mf LP light curves)

- ♣ The models are determined essentially by two free parameters: the shock compression and the shock direction (forward or reverse). The latter is expected to be important for time delay considerations.
- ♣ An extreme relativistic equation of state is assumed.
- ♣ A shock is introduced into the relativistic flow at $t=0$ at an oblique angle to the flow direction.
- ♣ Both simulated light curves and images are generated for comparison with the data.

Simulation from Radiative Transfer Calculations

Representative Light Curves

Specification of shock:

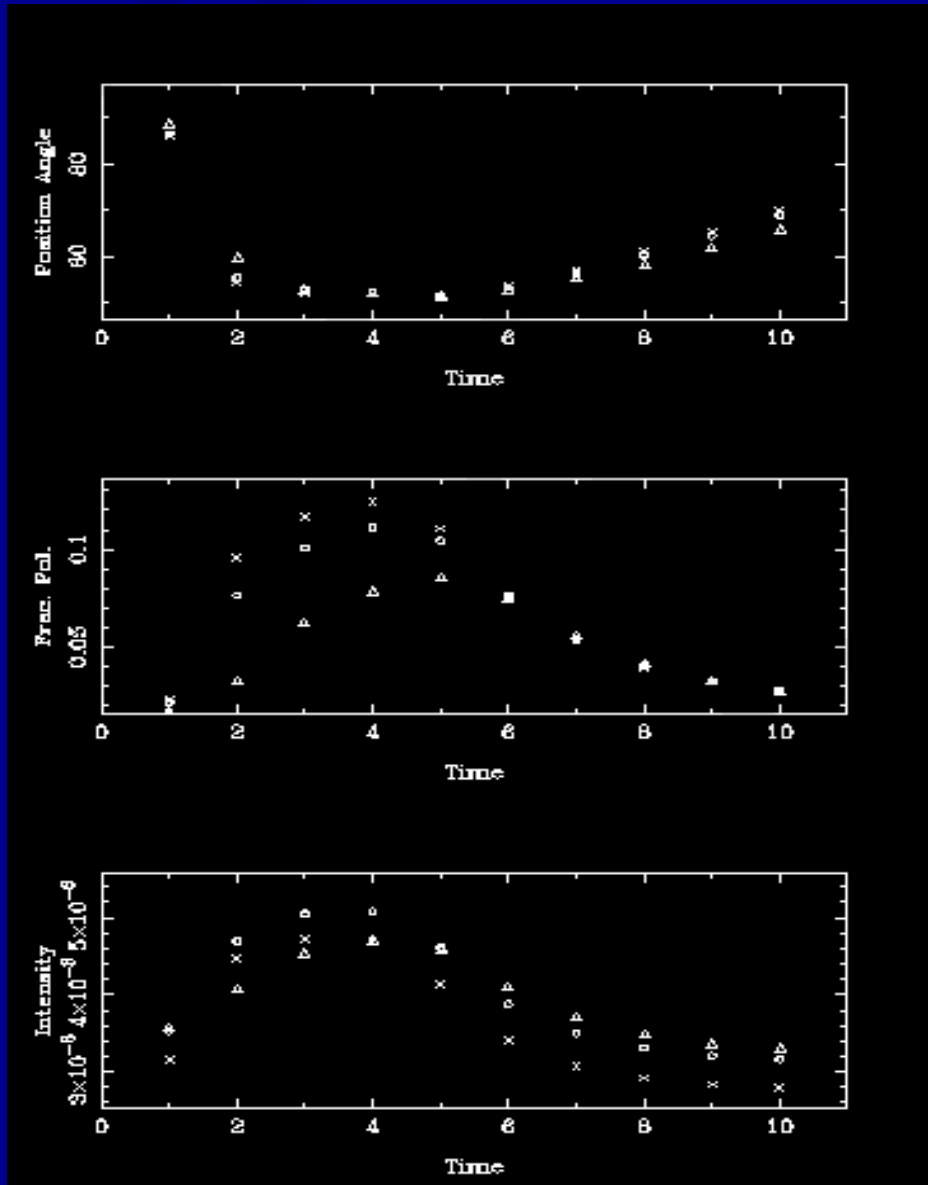
*Forward moving shock

*Compression=0.7

Lorentz factor of flow=2.5

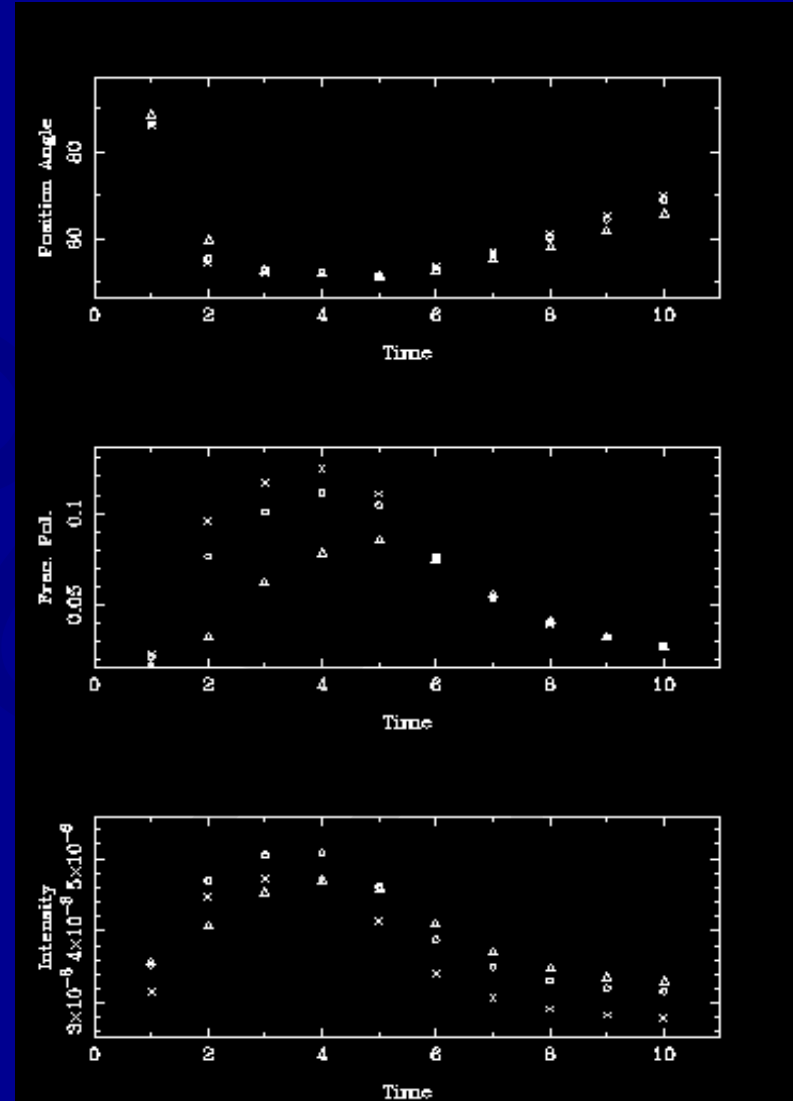
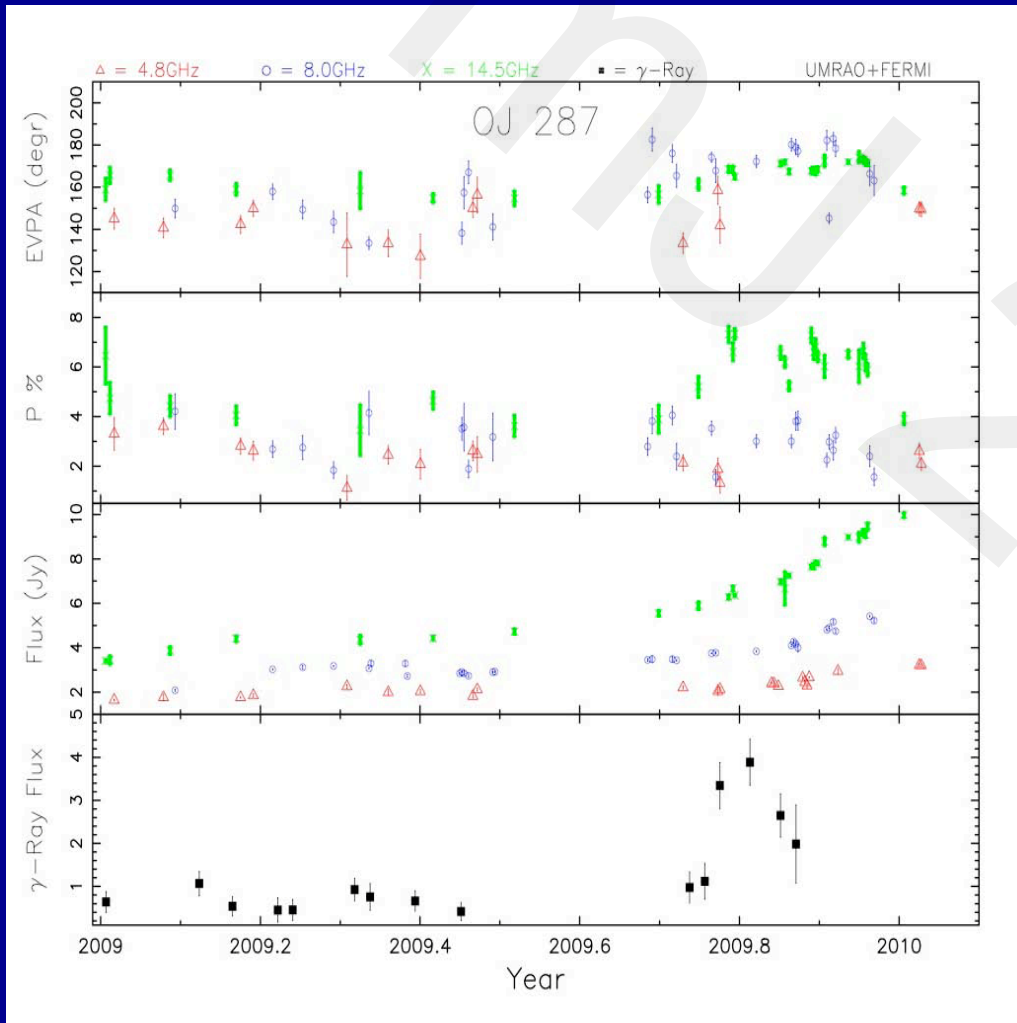
Lorentz factor of shock=6.7

Viewing angle=10 degrees

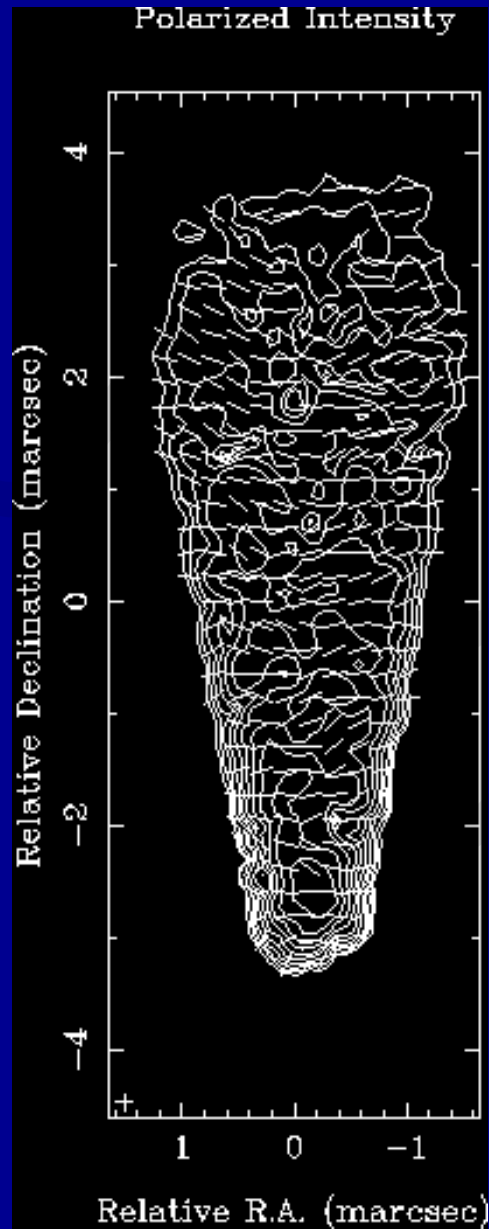


Primary Features of the light curves

1. Total flux outburst
2. Increase in linear polarization to near 10%
3. Swing in EVPA thru 40 degrees
4. Spectral behavior



Simulated structure images



Summary of Results Based on Combined Fermi and Single Dish Monitoring Data

- ♣ Flux-flux correlations obtained using time-averaged quasi-simultaneous data are highly significant. These argue for correlated broadband activity.
- ♣ Cross-correlations of the light curves show a variety of behavior patterns. Localization of the emitting region using these data must account for a number of factors potentially affecting the cross-correlation results.
- ♣ The association of rare, dramatic events in both bands can be easily identified, but in general the emission processes are different with respect to both noise process and characteristic time scale.
- ♣ Linear polarization monitoring verifies the presence of oblique shocks during gamma-ray flaring. In combination with modeling, the data can be used to identify jet conditions during gamma-ray flaring.

Future Work

- ♯ Deviations from the simple scenario of one mechanism/one site must be addressed:
 - ➔ rapid/hourly variability in 1510-089(Tavecchio et al.) vs evidence for origin near core (e.g. Pushkarev)
 - ➔ differences in class properties (Leon-Tavares)
- ♣ More detailed investigation of the character of the variability must be carried out as the Fermi data accumulates; if changes occur in **both** the radio and gamma-ray bands this would support the view that the emissions are causally related.
- ♯ Isolation of the specific conditions giving rise to gamma-ray flaring must be identified; these include searches for changes in jet properties from event to event in the same source.